

# Non-invasive imaging of global and regional cardiac function in pulmonary hypertension

Tim Crowe\*, Geeshath Jayasekera\* and Andrew J. Peacock

Cardiac and Vascular Imaging Group, Scottish Pulmonary Vascular Unit, Golden Jubilee National Hospital, Glasgow, UK

## Abstract

Pulmonary hypertension (PH) is a progressive illness characterized by elevated pulmonary artery pressure; however, the main cause of mortality in PH patients is right ventricular (RV) failure. Historically, improving the hemodynamics of pulmonary circulation was the focus of treatment; however, it is now evident that cardiac response to a given level of pulmonary hemodynamic overload is variable but plays an important role in the subsequent prognosis. Non-invasive tests of RV function to determine prognosis and response to treatment in patients with PH is essential. Although the right ventricle is the focus of attention, it is clear that cardiac interaction can cause left ventricular dysfunction, thus biventricular assessment is paramount. There is also focus on the atrial chambers in their contribution to cardiac function in PH. Furthermore, there is evidence of regional dysfunction of the two ventricles in PH, so it would be useful to understand both global and regional components of dysfunction. In order to understand global and regional cardiac function in PH, the most obvious non-invasive imaging techniques are echocardiography and cardiac magnetic resonance imaging (CMRI). Both techniques have their advantages and disadvantages. Echocardiography is widely available, relatively inexpensive, provides information regarding RV function, and can be used to estimate RV pressures. CMRI, although expensive and less accessible, is the gold standard of biventricular functional measurements. The advent of 3D echocardiography and techniques including strain analysis and stress echocardiography have improved the usefulness of echocardiography while new CMRI technology allows the measurement of strain and measuring cardiac function during stress including exercise. In this review, we have analyzed the advantages and disadvantages of the two techniques and discuss pre-existing and novel forms of analysis where echocardiography and CMRI can be used to examine atrial, ventricular, and interventricular function in patients with PH at rest and under stress.

## Keywords

pulmonary arterial hypertension, pulmonary hypertension, magnetic resonance imaging, echocardiography, right ventricle function and dysfunction

Date received: 28 March 2017; accepted: 11 October 2017

Pulmonary Circulation 2017; 8(1) 1–20

DOI: 10.1177/2045893217742000

## Introduction

Pulmonary hypertension (PH) is a progressive illness characterized by elevated pulmonary artery pressure (PAP); however, the main cause of mortality in patients with PH, especially in patients with pulmonary arterial hypertension (PAH) and chronic thromboembolic pulmonary hypertension (CTEPH), is right ventricular (RV) failure. Historically it was assumed that right heart dysfunction and subsequent failure was due to pulmonary hemodynamics; therefore, treatment of PH aimed to improve the hemodynamics of pulmonary circulation. It is now evident that cardiac

response to a given level of pulmonary hemodynamic overload is variable but plays an important role in the subsequent prognosis of these patients.

Cardiac function is usually assessed at the time of diagnosis along with pulmonary hemodynamics. Although right

\*Equal contributors.

Corresponding author:

Andrew J. Peacock, Scottish Pulmonary Vascular Unit, Golden Jubilee National Hospital, Agamemnon Street, Glasgow G12 8DY, UK.

Email: [apecock@udcf.gla.ac.uk](mailto:apecock@udcf.gla.ac.uk)



Creative Commons Non Commercial CC-BY-NC: This article is distributed under the terms of the Creative Commons Attribution-NonCommercial 4.0 License (<http://www.creativecommons.org/licenses/by-nc/4.0/>) which permits non-commercial use, reproduction and distribution of the work without further permission provided the original work is attributed as specified on the SAGE and Open Access pages (<https://us.sagepub.com/en-us/nam/open-access-at-sage>).

© The Author(s) 2017.  
Reprints and permissions:  
[sagepub.co.uk/journalsPermissions.nav](http://sagepub.co.uk/journalsPermissions.nav)  
[journals.sagepub.com/home/pul](http://journals.sagepub.com/home/pul)



heart catheterization (RHC) is essential for the diagnosis of PH, most PH units use a combination of 6-min walk test (6MWT), NT-proBNP, and clinical findings to determine prognosis and response to treatment. The reason RHC is not generally repeated regularly is, first, it is an invasive procedure requiring hospital admission and, second, although it tells us about pulmonary hemodynamics, it provides limited information about RV function and the consequences of RV dysfunction. In certain cases, RV function may improve without a consistent change in pulmonary hemodynamics; thus, an accurate understanding of RV function is important.

It is essential we have non-invasive tests of RV function to determine prognosis and response to treatment in patients with PH. Although the right ventricle is the focus of attention, it is clear that cardiac interaction can cause left ventricular (LV) dysfunction, thus biventricular structural and functional assessment is paramount. We must not forget the significance of the atrial chambers in their contribution to cardiac function and changes seen in PH. Furthermore, there is evidence of regional dysfunction of the right and the left ventricle in PH, so it would be useful to understand both global and regional components of dysfunction.

In order to understand regional and global cardiac function in PH, the most obvious non-invasive imaging techniques are those of echocardiography and cardiac magnetic resonance imaging (CMRI). Both techniques have their advantages and disadvantages. Echocardiography is widely available, relatively inexpensive, provides information regarding RV function, and can be used to estimate RV pressures. The advent of three-dimensional (3D) echocardiography and techniques, including strain analysis and stress echocardiography, will improve the usefulness of this modality. CMRI cannot be used to measure pressure, is less accessible and more expensive, but is the gold standard for determination of biventricular structure and function. New technology allows the measurement of strain using CMRI and recently there have been studies of CMRI measures of cardiac function during stress including exercise.

We believe that these techniques are complementary. In this review, we have analyzed the advantages and disadvantages of the two techniques and discuss pre-existing and novel forms of analysis where echocardiography and CMRI can be used to examine atrial, ventricular, and inter-ventricular function in patients with PH at rest and under stress.

## Cardiac function

In PH, the resistance in the pulmonary vasculature is raised. The right heart adapts to this by first hypertrophy and subsequently dilation.<sup>1</sup> The interaction between the right ventricle and pulmonary arteries is an interesting area of cardiac function assessment. Termed coupling, the ability of the right ventricle to accommodate increase in pulmonary vascular resistance (PVR) gives a measure of adaptability.

Coupling is typically measured by calculating the end-systolic elastance to arterial elastance ratio; ideally the right ventricle can adapt with increased contractility to maintain a ratio in the range of 1.5–2.0.<sup>2</sup> Outside of this ratio would imply loss of the coupling and lead to morphological adaptation with dilatation of the right ventricle. This process is indicative of failing RV function. Using non-invasive techniques to measure coupling is a challenge and typically achieved using MRI as discussed later. An echocardiographic technique was reported by Vanderpool et al. using Doppler echocardiography in three patients.<sup>3</sup> Furthermore, Guazzi et al. used non-invasive echocardiogram measurements to describe coupling in a large group of heart failure patients. They did not specifically measure elastance and their study is discussed further on in this review.<sup>4</sup>

Understanding myocardial fiber orientation of the right ventricle is key to understanding the effect of increased after-load on cardiac function. The right ventricle consists of deep myofibers running in a mainly longitudinal fashion and superficial fibers running more circumferentially.<sup>5</sup> The two-layer system causes a predominance of longitudinal contraction as the main contributor to ventricular emptying. The chamber acts as a bellows with the RV free wall closing in towards the intraventricular septum from the apex to basal region. A loss of this longitudinal function is seen in conditions of high PAP.<sup>6</sup> The LV myocardial composition differs and includes an oblique superficial layer, longitudinal deep layer, and a circumferential layer sandwiched between resulting in torsion as well as longitudinal contraction.<sup>5</sup>

While we acknowledge that other modalities including computed tomography (CT) and positron emission tomography (PET) exist as potential measures of cardiac function, the current focus of cardiac assessment in PH revolves around echocardiography and CMRI. Broadly CMRI leads in measures of RV function while echo leads in measures of intracardiac pressures. However, both modalities have advanced considerably in the last few years and here we will explore the actual and potential uses of the two techniques. Below we discuss regional and global cardiac function.

## Right ventricular function by echocardiography

Echocardiography has existed for over half a century, when Hertz and Edler identified the use of ultrasound to assess the heart.<sup>7</sup> Since the first echocardiogram, technology has moved forwards. Despite this, measurements that assess right heart function still use very basic echocardiography techniques. Roberts and Forfia provided a comprehensive review in this journal focused on assessment by Doppler echocardiography in 2011.<sup>8</sup> Other reviews in well-established publications also describe more recent developments in echocardiography.<sup>9,10</sup> We hope to combine tried and tested measurements with up-to-date developments in echocardiography.

The shape of the heart and its position in the human body can provide challenges to obtaining echocardiogram images for assessment of cardiac function. Fortunately, the nature of echocardiography allows multiple planar and sub-level views of the cardiac structures. Recommended protocols for assessing cardiac function exist, including those specific to PH.<sup>11,12</sup> There are multiple dimensional imaging options in echocardiography, from basic one-dimensional measurement using M-Mode through to 3D measurements collected over time making four-dimensional measurement of cardiac function possible.<sup>13,14</sup> Alongside this remains the ability of echocardiography to measure velocity by Doppler and therefore calculate pressure using the modified Bernoulli equation.<sup>15</sup> The development of software packages has further enhanced the measurements of cardiac function that can be obtained by echocardiography.<sup>16</sup> However, the need for greater standardization with these packages has already been highlighted.<sup>17</sup>

### *Right ventricular wall thickness and diameter*

Although a simple measurement, a wall thickness > 5 mm implies RV hypertrophy.<sup>18</sup> While this may not be specific for PH, it is nevertheless an abnormal measurement and reflects adaptation of cardiac function. As previously mentioned, in chronic PH, the initial response to increased PVR and associated afterload is hypertrophy of the right ventricular wall followed by dilatation. One study demonstrated that an end-diastolic diameter > 36.5 mm was associated with increased mortality (15.9 vs. 6.6 events/100 patient years).<sup>19</sup> However, this same study identified the benefit of adaptive hypertrophy, the group with right ventricle dilatation > 36.5 mm and RV wall thickness > 6.6 mm not showing a significant increase in mortality.

### *Right ventricular fractional area of change (RVFAC)*

RVFAC is calculated by the area of the right ventricle at end-diastole and end-systole. The equation is:

$$\text{End-diastolic area} - \text{end-systolic area} / \text{end-diastolic area}$$

This is typically mapped out from the two- or four-chamber view. It has been shown to correlate well,  $r = 0.80$ , with right ventricular ejection fraction (RVEF) calculated by MRI.<sup>20</sup> In a study looking at acute myocardial infarction (MI), each 5% reduction in RVFAC was associated with a 16% increase odds of mortality.<sup>21</sup> A value < 35% indicated RV systolic dysfunction.<sup>(11)</sup> As discussed elsewhere in this review, CMRI-measured RVEF is a strong indicator of cardiac function and prognosis; therefore, a value with close correlation to this has utility in its assessment. RVFAC does not take into account the complex shape of the right ventricle. It is therefore likely to show impaired accuracy against a 3D assessment which is discussed towards the end of this review.

### *Tricuspid annular plane systolic excursion (TAPSE)*

TAPSE is a basic but proven measurement of the right ventricle.<sup>22</sup> The measurement is taken using M-Mode and measures the peak systolic movement of the lateral tricuspid annular ring. The significance of TAPSE as a marker of RV function in PH was shown by Forfia in 2006.<sup>23</sup> A cutoff < 18 mm was associated with RV dysfunction and worse survival. Further review of this measurement in patients with PH has demonstrated a threefold increase in mortality with values < 15 mm.<sup>24</sup> TAPSE measurement continues to be used alongside others as a marker of RV dysfunction. There are, however, limitations in the use of TAPSE. In the assessment of cardiac function post pulmonary endarterectomy, TAPSE demonstrated significant worsening despite improvement in PVR.<sup>25</sup> In this setting, it was highlighted that the rocking motion of the heart contributed to TAPSE measurement, and this rocking motion was lost following pulmonary endarterectomy, hence the reduction in value. Another study looked at pseudo-normalized TAPSE in a group with RV dysfunction.<sup>26</sup> This again suggested contribution from rocking and also severe tricuspid regurgitation causing annular movement, affecting the value of TAPSE.

Sivak et al. looked at TAPSE in greater detail.<sup>27</sup> Total TAPSE was divided into two separate measurements, taken at two parts of the cardiac cycle. They termed these TAPSE<sub>RA</sub>, taken during RA contraction, and TAPSE<sub>RV</sub>, taken before RA contraction (Fig. 1). The value for TAPSE<sub>RA</sub> was similar between normal and PAH groups. TAPSE<sub>RV</sub> demonstrated impairment in the PAH group. TAPSE<sub>RA</sub>, however, contributed a greater percentage to overall TAPSE in the PAH group, 51% vs. 32.1% in the control group. Following treatment, and improvement in total TAPSE, TAPSE<sub>RA</sub> continued to contribute a significantly higher proportion of value to the overall measurement compared to the control values.

### *Right ventricular outflow tract (RVOT)*

The RVOT is the communication between the RV and the pulmonary vasculature. It is cylindrical in shape and changes diameter during the cardiac cycle. In PH, it becomes dilated, although its usefulness in assessing cardiac function is less well explored. One study looked at measurement of the systolic excursion of the RV outflow tract anterior wall in a population group with multi-modal causes of PH.<sup>28</sup> The measurement was taken in the short axis at the level of the aortic valve. A value < 6 mm was associated with worse survival at one year, 63% vs. 84% ( $P = 0.004$ ). Another study also used a mixed population group to assess systolic wall excursion and identified significant strong correlations ( $r = 0.81$ ) with TAPSE and RVFAC.<sup>29</sup> Fractional shortening is the RVOT measurement of the RVOT diameter in diastole minus RVOT diameter in systole divided by the RVOT diameter in diastole. Lindqvist et al. had previously demonstrated impairment of this value in a group of patients with PH.<sup>30</sup>

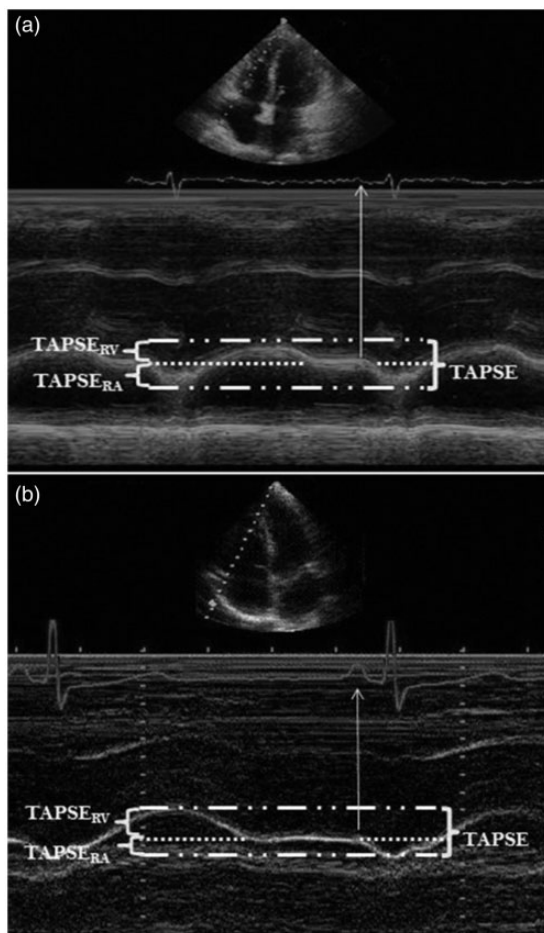


**Fig. 1.** TAPSE in greater detail. Total TAPSE was divided into two separate measurements, taken at two parts of the cardiac cycle, termed TAPSE<sub>RA</sub>, taken during RA contraction, and TAPSE<sub>RV</sub>, taken before RA contraction. Taken from Sivak et al.<sup>26</sup>

**Doppler measurement: tricuspid regurgitant velocity (TRV), tricuspid regurgitant pressure gradient (TRPG), right ventricular systolic pressure (RVSP), pulmonary arterial systolic pressure (PASP), and S' wave velocity**

There are entire review articles based on Doppler measurements of RV function.<sup>8</sup> TRV is a Doppler measurement taken across the tricuspid valve. In PH and associated RV remodeling due to increased afterload, functional tricuspid regurgitation takes place. This measurement is still classically looked at in the screening assessment of patients with suspected PH.<sup>9</sup> TRV can be calculated to TRPG using the Bernoulli equation,  $\text{pressure} = 4V^2$ . Estimation of right atrial pressure by inferior vena cava assessment can then be added to TRPG to calculate RVSP.<sup>11</sup> In the absence of pulmonary valve stenosis, the resultant pressure calculation is equivalent to PASP. While this aids in the assessment of PH, it does not necessarily reflect RV function.<sup>31</sup> Inherently, the value multiplies any error of measurement, the right

atrial pressure is only an estimate, Doppler measurements are angle-dependent, and a failing right heart may generate less TRV from reduced contraction and greater annular dilatation. Fisher et al. measured the accuracy of TRV against right heart catheter data and identified inaccuracies > 10 mmHg in 48% of cases.<sup>31</sup> Similar numbers of cases were over- or underestimated, but the discrepancy from the invasive measurement was larger when underestimated. Despite this, more recently one study looked at longitudinal assessment of tricuspid valve regurgitation.<sup>32</sup> This study assessed three groups: those who progressed from mild to moderate regurgitation; those that remained mild; and those that regressed from moderate to mild. The data showed that those whose assessment of TRV deteriorated had the worst mortality at three years of 88%. This compared to those with stable function and those that improved, who had three-year mortality figures of 39% and 22%, respectively. This study did not assess those with severe TR which may suggest a limitation in use of TRV in severe disease. S' wave velocity of the tricuspid annulus is another Doppler tissue measurement (Fig. 2). Taken in the four-chamber view, a measurement < 11.5 cm/s predicted RV dysfunction in a population with LV failure.<sup>33</sup> A value < 10 cm/s is now recommended as a measure of impaired function in echocardiography guidelines for assessment of the right ventricle.<sup>18,34</sup>

### Myocardial performance index (Tei index)

The Tei index provides a measure of both diastolic and systolic function of the ventricle. The equation below shows the calculation. The sum of isovolumetric contraction and relaxation times can be calculated by measuring the stop and start of tricuspid inflow and subtracting the ejection time (Fig. 2):

$$\frac{(\text{isovolumetric contraction time} + \text{isovolumetric relaxation time})}{\text{right ventricular ejection time}}$$

Using this performance index to assess the right ventricle in PH was described by Tei in 1996.<sup>35</sup> In their model, they measured tricuspid inflow in the four-chamber view along with RV ejection time. In the PH group, the index was increased at 0.93 vs. 0.28 in the control group. Further analysis showed better prognosis in the PH group with index < 0.83.<sup>36</sup> An animal study investigating the effect of loading on the index demonstrated clear load dependency.<sup>37</sup> Increased afterload and reduced preload increased the index, the authors concluding the index could not be used to assess change in ventricular contractile function.

The measurements discussed above are well established as measures of cardiac function in PH. Echocardiography pre-dates the advent of MRI; however, CMRI has taken the lead in imaging quality. Below we discuss established MRI measures of RV function.



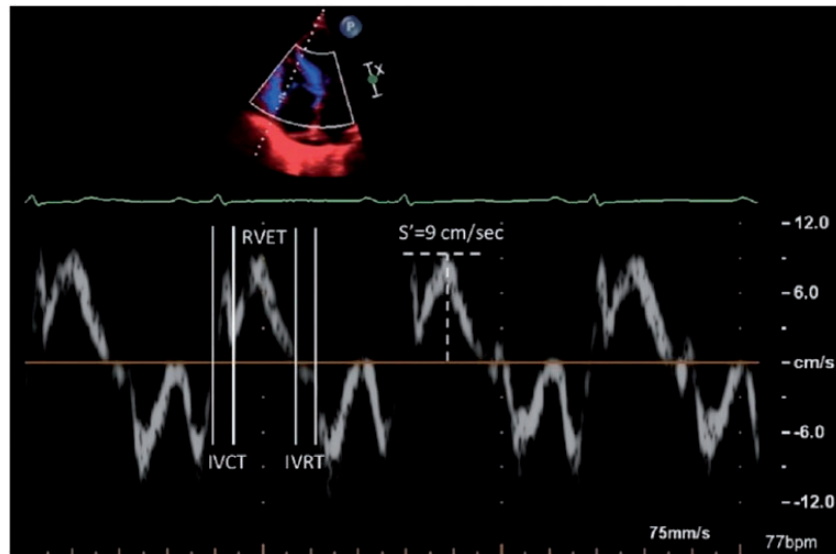


**Fig. 2.** Tei index or the myocardial performance index which is calculated by measuring the time between cessation and start of tricuspid inflow and the ejection time of the right ventricle, and  $S'$  wave velocity of the RV free wall. Image taken from Roberts and Forfia.<sup>8</sup>

### Right ventricular function by CMRI

CMRI is a non-invasive imaging tool and provides high-resolution 3D images of the heart. Short axis stacks are used to reconstruct a 3D image of the right and the left ventricle and ventricular volumes and wall mass can be measured covering the entire cardiac cycle. Endocardial and epicardial contours are drawn at end-diastole and end-systole during post processing of images and ventricular volumes are calculated using the “Simpsons rule,” which takes the sum of individual slice volumes and the interslice gap into account. From the volume changes of the right ventricle over time, systolic function can be calculated. New software solutions with semi-automatic analysis have resulted in decreased post-processing times. The inter-study reproducibility and accuracy of CMRI measurements using a semi-automatic analysis have been validated in several reports. However, interstudy reproducibility of the right ventricle measurements is lower than for the LV. Endocardial boundary delineation of the thin-walled RV is more complicated compared to LV and basal slice definition of the RV in short axis view is more difficult than the LV. This is important in the interpretation of studies using CMRI RV measurements as an endpoint.<sup>38,39</sup> Velocity encoded cine MR images are used to quantify pulmonary artery flow. The aorta flow can be measured in the same plane and the ratio of pulmonary artery: aorta flow ( $Q_p:Q_s$ ) and vice versa can be used to assess intra-cardiac shunts. Beerbaum et al. concluded that the calculation of  $Q_p:Q_s$  by cardiac MR to be quick, safe, and reliable in children with cardiac defects.<sup>40</sup> The ability to assess RV systolic function by conventional echocardiography based on volume calculations is limited. Although contrast-enhanced 3D echocardiography has become available recently and has

shown to be useful in assessing RV mass and RVEF, CMRI remains the gold standard.<sup>41</sup>

A large number of studies using CMRI in patients with PAH have been published. Many CMR measures have shown to be strongly predictive of mortality and survival thus offering potential for monitoring and assessing response to treatment. Of these, stroke volume (SV) is recognized as the key MR prognostic measure in PAH patients. Van Wolferen et al. investigated the prognostic significance of a variety of LV and RV structural and functional measurements in patients with idiopathic PAH (IPAH).<sup>42</sup> They showed that a low SV at baseline to be a predictor of poor prognosis.<sup>42</sup> They also showed that SV rather than cardiac index to have a stronger correlation with prognosis in these patients, possibly explained by the fact that there may be compensatory increase in heart rate which will flaw the relationship between cardiac output and prognosis. The results in this study also suggested that a decrease in SV during treatment to be an indicator of treatment failure. Although results were comparable when SV were measured by CMRI or with the Fick method, CMRI underestimated SV. This is probably explained by turbulent blood flow patterns observed in the main pulmonary artery. This was evident both at baseline and at follow-up. In a large single-center cohort of patients with systemic sclerosis-associated PAH, stroke volume index (SVI) was a strong predictor of survival. There was twofold increased risk of mortality in patients with a  $SVI < 30 \text{ mL/m}^2$ .<sup>43</sup> Van Wolferen et al. evaluated 111 patients at baseline and at one-year follow-up to identify a minimally important difference in SV in patients with PH. They used both an anchor-based method (using 6MWT as anchor) and a distribution-based method and showed that a 10-mL change in SV during follow-up should be considered as clinically relevant.<sup>44</sup> However,

relatively small changes in RV variables by CMRI measurements need to be interpreted with caution due to the complex geometry and relatively weaker reproducibility of these measurements compared to LV.

RVEF is also an important prognostic factor in patients with PH and is poorly derived by conventional echocardiography. A study in a large group of WHO group 1 patients with PAH, RVEF measured at baseline was a better predictor of mortality compared to PVR. They showed, in patients who are on PAH targeted therapy, that RV function can deteriorate despite reduction in PVR, which occurred in 25% of the patients. They showed that the deterioration of RVEF was associated with poor outcome independent of any changes of PVR. They hypothesized that the deterioration in RVEF could be explained by pulmonary pressures and subsequently ventricular wall tension that was unaltered after medical treatment despite a fall in PVR. This study emphasized the importance of monitoring RV function during the course of the disease.<sup>45</sup>

RV end-diastolic volume is another predictor of prognosis in PAH. Kaplan–Meier survival analysis in a study by Van Wolferen et al. demonstrated that patients with a RV end-diastolic volume index (RVEDVI)  $< 84 \text{ mL/m}^2$  at diagnosis had a significantly better survival compared to those with a RVEDVI of  $84 \text{ mL/m}^2$  or more.<sup>42</sup> A further study by Yamada et al. showed that an increased RVEDI predicted both hospitalization and mortality in patients with IPAH but could not establish a significant difference between the aforementioned two groups in the previous study.<sup>46</sup> In a study by Mauritz et al., CMRI defined geometric changes during the development of RV failure.<sup>47</sup> They identified certain CMRI-derived geometric characteristics that defined non-survivors (survival  $< 5$  years) at the beginning of the study and at one-year follow-up. They identified that the RV longitudinal shortening (distance change between end-diastole and end-systole of the tricuspid annulus to apex distance) and transverse shortening (change between end-diastole and end-systole of the RV free wall to septal distance) are already reduced at baseline in non survivors, that transverse shortening further declines over time while longitudinal shortening and RV free wall motion stay the same and that the end-stage decline in RV function is due to progressive leftward septal displacement rather than further changes in RV free wall transverse or longitudinal displacement. The authors concluded that although there is a parallel decline in longitudinal and transverse shortening during progressive RV failure, a floor effect is reached for longitudinal shortening. Further RV failure causes progressive leftward septal displacement and as transverse shortening incorporates both free wall and septal motion, it could be used as a variable of monitoring RV failure. They identified that the RVFAC, which combines the effect of both transverse and longitudinal shortening (calculated by  $= 100 \times [(RVED \text{ area} - RVES \text{ area}) / RVED \text{ area}]$ ) correlates well with RVEF. They identified that a decline in RVFAC to be an accurate measure of RV failure in patients with severe PAH (Fig. 3).

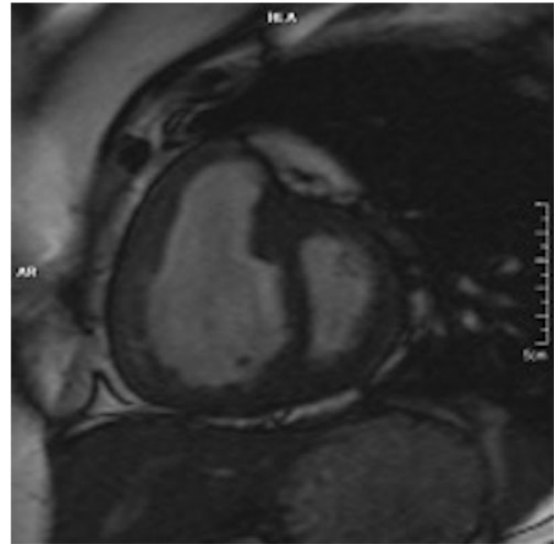


**Fig. 3.** CMRI: short-axis view of a 33-year-old woman with exertional dyspnea. There is RV dilatation and hypertrophy, and interventricular septal bowing.

### Phase contrast MRI

Blood flow of the main pulmonary artery can be measured with phase contrast imaging with gradient echo imaging with velocity encoding gradients. Various measurements such as average velocity, peak velocity, anterograde and retrograde flow can be determined. Sanz et al. demonstrated that average velocity of the blood flow in PA to correlate with invasive pressure measurements (systolic PAP  $r = -0.76$ , mean pulmonary artery pressure [mPAP]  $r = -0.73$ , and PVR index  $r = -0.86$ ).<sup>48</sup> Average velocity with a cutoff value of  $11.7 \text{ cm/s}$  was 92.9% sensitive and 82.4% specific to detect PH. Mousseaux et al. demonstrated good correlations between right heart catheter measurements and MR velocity encoded image derived flow measurements, enabling distinction of individuals with high PVR from normal PVR.<sup>49</sup> Relative onset of time (ROT) of retrograde flow in the main pulmonary artery (relative to cardiac cycle duration) were determined in a study by Helderma et al., consisting of 38 PAH patients.<sup>50</sup> A ROT of 0.25 distinguished PAH patients from non-PH patients, demonstrating that early onset of retrograde flow to be characteristic of PAH.

### Pulmonary artery stiffness and pulsatility

Pulmonary arterial elasticity is an important factor determining the relationship between the right ventricle and the PA, RV–PA coupling. A study was conducted to evaluate pulmonary arterial stiffness in patients with PH, exercise-induced PH, and no PH. Various indices of PA stiffness were studied. These included: (1) relative change in lumen area during cardiac cycle (pulsatility); (2) absolute change in lumen area for a given pressure (compliance); (3) change in volume associated with a given pressure (capacitance);

(4) relative change in lumen area for a given pressure (distensibility); (5) pressure change driving a relative increase in lumen area (elastic modulus); and (6) slope of function between distending arterial pressure and arterial distension (stiffness index beta). Patients with exercise-induced PH had lower median compliance and capacitance than patients with no PH. The aforementioned different measures of PA stiffness showed significant correlation with PA pressures ( $r^2=0.27-0.73$ ). The authors concluded that PA stiffness occurs early in PH even when overt pressure elevations are not present at rest.<sup>51</sup>

### **RV-PA coupling**

The gold standard measure of RV systolic functional adaptation to changes in afterload is to measure end-systolic elastance (Ees), which is derived by dividing end-systolic pressure (ESP) by end-systolic volume (ESV), corrected for arterial elastance (Ea) (SV/ESP). This load-independent measure of RV-PA coupling defines matching of RV contractility to afterload. Although this requires instantaneous measurements of RV pressure and volume which is not practical, this can be simplified for pressure and expressed either as a SV/ESV ratio (the volume method) or simplified for volume and expressed as RV maximum pressure divided by mPAP - 1 (the pressure method). In a study of 140 treatment-naïve patients by Brewis et al., RV-PA coupling measurements by volume method (SV/ESV) predicted outcome; however, there were no added benefits of RV-PA coupling measurements by the pressure method.<sup>52</sup>

As previously mentioned, an alternative descriptor of coupling has been analyzed in echocardiography.<sup>4</sup> In a study of 459 patients with heart failure, TAPSE/PASP ratio was used as a measure of cardiac and pulmonary arterial coupling. The group with the lowest ratio, that is low TAPSE with high PASP, had greater risk of adverse events and most impaired clinical function. Although the authors termed this study ventriculo-arterial coupling, their measurements did not calculate elastance within the ventricle or pulmonary vasculature.

### **Left ventricular assessment by echocardiography and CMRI**

In a multicenter study prospectively assessing the use of CMRI before and during PAH disease-specific treatment, Peacock et al. demonstrated the importance of including both left-sided and right-sided variables when determining cardiac function.<sup>53</sup> In the EURO-MR study they highlighted that LV end-diastolic volume (LVEDV) is more closely related to stroke volume than RV end-end diastolic volume. From previous studies, it was known that poor LV output in PH patients was due to poor LV filling which was a consequence of prolonged RV contraction time. This contributed to a decreased stroke volume; thus, LVEDV reflected both the stroke volume and RV contraction time.

Elevated RV pressure causes bowing of the interventricular septum in patients with PH. This causes a deformation of the left ventricle to a “D” shape. Roeleveld et al. observed that maximal distortion of normal septal shape to be during RV relaxation and found systolic PAP to be proportional to septal curvature ( $r=0.77$ ,  $P<0.001$ ).<sup>54</sup> Dellegrottaglie et al. defined curvature ratio as ( $C_{IVS}/C_{FW}$ ), by interventricular septal curvature ( $C_{IVS}$ ) and LV free wall curvature ( $C_{FW}$ ), which were measured at end-systole.<sup>55</sup> These were used to derive the curvature ratio ( $C_{IVS}/C_{FW}$ ). They concluded that in patients clinically known to have or suspected of having PH, CMRI-derived curvature ratio, as compared with RHC measurement, was an accurate and reproducible index for estimation of RVSP. Beyar et al. demonstrated that interventricular septal bowing is present in an animal model when the pressure differential (RV pressure-LV pressure) exceeds 5 mmHg and a strong association between interventricular septal curvature and the RV-LV pressure gradient was demonstrated as RV pressure increases.<sup>56</sup>

### **Left ventricular eccentricity index by echocardiography**

This measurement of the LV can be taken in end-systole or end-diastole using the short-axis view at the mid-papillary level. The calculation divides the measurement of the LV cavity parallel to the interventricular septum by the perpendicular measurement. In PH, an increase in the diastolic measurement suggests increased RV volume, while an increase in diastolic and systolic measurement implies increased RV pressure.<sup>57</sup> Puwanant et al. demonstrated an end-diastolic value of 1.24 vs. 0.96 in PH compared to controls and end-systolic value of 1.55 vs. 1.03, respectively.<sup>58</sup> In another study, an end-diastolic value  $\geq 1.7$  was associated with a higher number of events (mortality or transplant) in a PH group.<sup>24</sup>

While it is noted that the right ventricle is the most widely studied of the chambers in PH, focus has started to move to the left ventricle. As described above, there is now evidence demonstrating this is also impaired in function in this disease process. Further to this, the atrial chambers offer valuable information when measuring cardiac function in PH and this is explored below.

### **Atrial assessment by echocardiography and CMRI**

#### **Right atrium (RA) by echocardiography**

Measurement of the RA is not a particularly recent development, but has perhaps fallen out of favor. The RA has three distinct functions, employed at different stages of the cardiac cycle: reservoir function during ventricular systole; conduit function during initial ventricular filling; and active function at end ventricular diastole. In 2008, Willens et al. looked at RA function in PH patients vs. controls.<sup>59</sup> Patients with PH were noted to have increased filling

capacity, reflecting reservoir function; poorer passive RV filling, reflecting conduit function; and better active function at the end of diastole. Before this, Lambertz et al., in 1985, had already concluded increased right atrial active function contributed to improved RV filling in RV pressure overload.<sup>60</sup> In addition, a study using a dog model also demonstrated elevated RV pressure was associated with increased atrial reservoir and active function, suggested to be a compensatory mechanism in elevated RV pressure.<sup>61</sup> More recently, advances with strain analysis of the RA have furthered our knowledge of atrial function, and this is discussed later in this review.

### *Left atrium (LA) by CMRI*

Determination of LA size is primarily used to exclude PH due to left-sided cardiac dysfunction. PH in HfPEF (heart failure with preserved ejection fraction) is venous in origin and causes LA dilatation. In a study by Crawley et al., LA volume was determined using standard two- and four-chamber CMRI views and the biplane area-length method, and indexed to the body surface area. LA volume was significantly lower in IPAH (and indeed lower than normal) compared with HfPEF ( $24 \pm 9 \text{ mL/m}^2$  vs.  $66 \pm 19 \text{ mL/m}^2$ ,  $P < 0.0001$ ). Using a LA volume threshold of  $43 \text{ mL/m}^2$  as the cutoff, they could distinguish IPAH from HfPEF with 97% sensitivity and 100% specificity.<sup>62</sup>

### **Developing areas**

The second part of this review discusses the developing areas of non-invasive imaging of cardiac function. This area is constantly evolving as technological developments facilitate new applications in measurement.

### **Strain and strain rate by echocardiography**

Echocardiography produces grayscale images transposed from the reflection of sound waves. The images produced are typically captured over the length of at least one cardiac cycle. This allows visual analysis of the movement of cardiac structures throughout the cardiac cycle. The change in shape of the myocardial walls with contraction or relaxation is termed deformation. Deformation can be measured by strain analysis.<sup>63</sup>

Strain classically has two descriptors, Lagrangian and Natural. Lagrangian strain is the change in length from starting point, usually termed  $L_o$ , to endpoint, typically termed  $L$ , and divided by starting point  $L_o$ . If the length reduces at point  $L$ , it is a negative measurement. If the length increases at point  $L$ , it is a positive measurement. We must note that strain can be measured between any two moments within any episode of deformation and this is termed natural strain. Lagrangian strain is the measurement usually employed in the assessment of cardiac wall movement. Myocardial strain analysis typically accepts

end-diastole (maximal ventricular size) as  $L_o$ . Therefore, all measurements are fundamentally negative as the wall contracts and then relaxes, returning to point  $L_o$ . The more negative the value the greater the deformation.

Traditionally strain measures the change in one dimension of measurement. In echocardiography, strain has been assessed by Doppler imaging and speckle tracking method. The latter is described in more detail below. Doppler imaging requires identification of small regions of interest (ROI) in the myocardial wall. Changes in velocity of this ROI can be mapped through the cardiac cycle. Then by adjusting for temporal and spatial resolution, strain can be calculated. In recent years, this process has become superseded by the speckle tracking method.

The addition of timing to the measurement of strain allows the strain rate to be calculated. Strain rate is calculated by  $\Delta L/\Delta t$ . Whereas Lagrangian strain is the measurement from baseline, the rate can be measured continuously throughout the cardiac cycle. Systolic measurements of strain and strain rate are typically reported in studies looking at strain as a measure of cardiac function. Strain rates, however, also provide early and late diastolic peak values, providing insight into diastolic function.

### *Speckle tracking echocardiography*

The principle of speckle tracking in echocardiography has existed for over a decade. It remains an active area of interest for research in RV function. Speckle is the term given to the grayscale pixilation pattern created by the reflection of sound waves at an interface. The imperfection of a surface creates a unique reflection and therefore fingerprint of pixels at that region. This pixel fingerprint can subsequently be tracked across the cardiac cycle from image to image. By tracking many pixels across a ROI, the deformation of the tracked structure can be measured, thus strain can be calculated along the entire ROI. The software available not only assesses the whole wall, but can be separated into segments. The origin of speckle tracking in LV assessment is of particular use when identifying regional wall movement abnormalities in cardiac ischemia. The application of speckle tracking strain analysis in RV function is not to identify ischemic myocardium, but allows measurement of global and regional wall movement.

The analysis by speckle tracking is typically performed offline. Unlike Doppler imaging, speckle tracking is not dependent on angle; however, it does require adequate frame rates to allow tracking and an adequate grayscale. Speckle tracking is also dependent on inclusion of the whole ventricular wall throughout the cardiac cycle. Measurement of deformation can be made in three planes: longitudinally; circumferentially; and radially. Imaging the latter two in the right ventricle by two-dimensional (2D) imaging is challenging. As discussed later, developments in 3D echocardiography assists with this limitation. Longitudinal strain of the RV free wall is the measurement often reported in the literature (Fig. 4).





Fig. 4. Speckle tracking echocardiography measuring longitudinal RV strain in a patient with IPAH.

### Strain and strain rate in cardiac function

Strain analysis through tracking has been reported since 2004.<sup>64,65</sup> In these studies, impairment was demonstrated in the left ventricle of post-MI hearts. The use of speckle tracking echocardiography to analyze strain has been validated by sonomicrometry and MRI tagging.<sup>66,67</sup> Using a dog model and LV measurements, correlation of longitudinal systolic strain between speckle tracking and sonomicrometry was significant ( $r=0.90$ ). Correlation with human participants by MRI tagging of the long axis was also significant ( $r=0.87$ ).<sup>67</sup>

When assessing RV function by strain, both tissue Doppler imaging and speckle tracking have been studied for over a decade.<sup>68,69</sup> Rajdev et al. demonstrated the use of tissue Doppler imaging to assess strain of the RV and LV free walls and the intraventricular septum. They showed a reduction in strain across all ventricular walls in the PH group vs. controls. They also demonstrated variation in strain at each segment—basal, mid, and apical. In addition, they measured peak diastolic values with strain rates and were able to identify differences when grouped by RVEF. They did, however, report inter-observer variability in the range of  $11.2\text{--}26.6\% \pm 30.9$  and intra-observer variability of  $13.6\text{--}18.2\% \pm 13$ . Borges et al. looked at tissue Doppler imaging and speckle tracking in patients with PAH and controls.<sup>69</sup> They also determined response to treatment. Borges et al. demonstrated significant changes in strain measurements between pre- and post-treatment groups as well as between the pre-treatment group and healthy controls. Both tissue Doppler measurements and speckle tracking showed significance between groups, although were not compared against each other. Teske et al. did compare the two techniques for measuring RV free wall strain and reported similar observer variabilities and moderate

correlation in values of strain and strain rate, further details of their studies are documented below.<sup>70</sup>

Peak systolic longitudinal strain of the right ventricle has become much more established as a measure of cardiac function in PH. Filusch et al. also used tissue Doppler imaging to measure peak systolic strain and strain rate of the RV free wall in controls and IPAH patients. They demonstrated strain and strain rate correlated with PVR, mPAP, CO, TAPSE, Tei index, NT-proBNP, and 6MWT.<sup>71</sup> This would imply strain may have a value as a continuous variable of cardiac function, although in current guidelines, a value less negative than  $-20\%$  (i.e. smaller measure of strain) is accepted as a cutoff measure of impairment.<sup>11</sup> Meanwhile, Sachdev et al. looked at a PAH group and demonstrated impaired RV free wall peak systolic longitudinal strain and strain rates, where average strain was  $-15.5\%$  and strain rate  $-0.80\text{ s}^{-1}$ .<sup>72</sup> Comparing those with a strain less negative than  $-12.5\%$  compared to more negative than  $-20\%$  showed four-year mortality of 93% vs. 39%, respectively. Regarding strain rate, a value less negative than  $-0.7\text{ s}^{-1}$  was associated with worsened disease progression and mortality.

Haeck et al. also looked at peak systolic longitudinal strain of the RV free wall in a PH group.<sup>73</sup> They found the group with a strain value less negative than  $-19\%$  was associated with an impaired survival over a five-year period of 55%. They also identified a higher NYHA function class, increased diuretic use, larger RV areas with reduced RVFAC, and lower TAPSE in this group.

Global strain assessments of the right ventricle, including measurement of the intraventricular septum and free wall, have also been studied.<sup>74–76</sup> In a group of PH and control participants, global peak systolic RV longitudinal strain (GRVLS) was reduced in the PH group ( $-15.6\%$  vs.  $-23.8\%$ ).<sup>74</sup> In another PAH group, a GLRVS less negative

than  $-15.5\%$  was associated with reduced event free time and total survival.<sup>76</sup> In 2015, Park and Kusunose also looked at global peak systolic RV longitudinal strain and isolated free wall strain before and after therapy for PAH.<sup>74</sup> They showed improvement in longitudinal strain measurements and moderate correlation with change in strain and mPAP. More recently, a study looking at longitudinal RV free wall strain against other echocardiogram parameters and pulmonary pressures showed a strain value of  $-19.26\%$  was diagnostic of  $\text{mPAP} \geq 45 \text{ mmHg}$  with a sensitivity of  $83.9\%$  and a specificity of  $73.4\%$ .<sup>77</sup>

As previously described, segmental analysis of the myocardial walls is possible, although has been less well reported in literature.<sup>70,78</sup> In these studies, Teske et al. used tissue Doppler and speckle tracking methods to measure strain and strain rates in controls, athletes, and elite athletes. In part of their study, they divided the group by controls and athletes with RV dilatation.<sup>78</sup> The athletes with dilatation had average RV free wall basal peak systolic strain values of  $-20.9\%$  by TDE and  $-22.6\%$  by speckle tracking with strain rates of  $-1.23/\text{s}$  and  $-1.33/\text{s}$ , respectively. For the same region, the control group had strain values of  $-24.5\%$  by TDE and  $-25.5\%$  by speckle tracking with strain rates of  $-1.50/\text{s}$  and  $-1.62/\text{s}$ , respectively.

In a group of chronic thromboembolic patients followed up after pulmonary endarterectomy (PEA) surgery, there was unexpected reduction in peak systolic strain of the basal segment; average values reduced to  $-18.9\%$  from  $-24.3\%$ .<sup>79</sup> Time to peak strain was also shortened. The echocardiograms were on average performed nine days following surgery and the authors hypothesized the consequence of ventricular ischemia or stunning as a cause for the worsening basal function. Consideration would also need to be given to time for cardiac remodeling. This would be supported by a study on patients who underwent balloon pulmonary angioplasty that showed an average improvement in strain globally of  $-4.4\%$  when reassessed three months after the procedure.<sup>80</sup> In a study looking at RV global, free wall, and segmental analysis in PH patients, Li et al. were able to demonstrate reduced strain and strain rate function across the walls and within segments when compared to controls.<sup>81</sup> They also showed correlation with global strain and strain rates of the RV and RVEF measured by CMR of  $r=0.693$  and  $0.560$ , respectively.

### *Right atrial strain*

Using speckle tracking, a few studies have looked at right atrial strain measurements. Roca et al. measured strain and strain rate across the right atrial wall.<sup>82</sup> Longitudinal RA strain was taken as a measure of reservoir function, early diastolic strain rate as a measure of conduit function, and late diastolic strain rate as a measure of active function. They analyzed 65 PAH patients and 30 controls. Longitudinal RA strain and early diastolic strain rate were both impaired in PH patients. Longitudinal RA strain

showed significant correlation with several markers, particularly TAPSE and RV free wall strain. Late diastolic strain rate of the RA showed no significant impairment when compared with controls, but did show greater contribution to emptying of the RA. D'Andrea et al. assessed RA strain at rest and exercise.<sup>83</sup> Although they did not use a PH population group, they were able to compare controls with patients with systemic sclerosis. Using a supine bike model, RA strain was recorded along with more traditional echo parameters. D'Andrea et al. identified impaired RA strain in both the lateral and septal atrial walls when compared to controls both at rest and exercise. They also identified correlation between RA strain and LV stroke volume. They suggested RA strain may be an early indicator of diastolic cardiac impairment. The analysis of RA strain has shown use in other areas of assessment of PH. One study of PH patients demonstrated that the sum of the reservoir, conduit, and contraction strain values correlated well with mPAP ( $r^2=0.56$ ).<sup>84</sup>

### *Right ventricular dyssynchrony*

This assessment of cardiac function by strain allows recording across the timing of the cardiac cycle. This utility has been adapted to calculate intra-ventricular dyssynchrony.<sup>85</sup> This is calculated by taking the SD of the time to peak strain measured across a chosen number of chamber wall segments. SD4 models, using the basal and mid segments of the free wall and septum, and SD6 models, including the apical segments as well, are described in studies on dyssynchrony. The higher the SD, the greater the dyssynchrony. Haeck et al. used the six-segment model to assess the right and left ventricles in a group with PH.<sup>86</sup> They demonstrated a  $\text{RV-SD6} > 49 \text{ ms}$  was associated with worse clinical function. The correlation of RV dyssynchrony with LV dyssynchrony was  $0.55$ , suggesting the presence of inter-ventricular dependence. Badagliacca et al. used a  $\text{RV-SD4}$  model in their assessments of RV dyssynchrony.<sup>87,88</sup> In these two studies, values  $> 18\text{--}19 \text{ ms}$  were associated with worse WHO functional class (WHO FC), 6-min walk distance, RV remodeling, and impaired RV hemodynamics. It is clear to see that dyssynchrony remains an area of ongoing interest.

### *Torsion of the left ventricle*

Impairment of torsion was demonstrated by Helle Valle et al. using a dog model and sonomicrometry in 2005.<sup>66</sup> Both Helle Valle et al. and Notomi et al. also compared torsion by echocardiography measures against MRI tagging, with the latter using tissue Doppler imaging and speckle tracking.<sup>89</sup> During LV systole, and when viewed from the apex, the apical segment rotates in an anti-clockwise direction, while the basal segment moves clockwise. This effect in both segments was enhanced by dobutamine administration, while only apical twist was

impaired by myocardial ischemia. Puwanant et al. demonstrated an impaired torsion in PH compared to controls,  $9.6^\circ$  vs.  $14.9^\circ$ , but preserved untwisting rates.<sup>58</sup> They suggested raised RV pressure caused septal flattening and bowing into the left ventricle impairing the ability of the left ventricle to torque. While LV torsion continues to be studied in other conditions, there are limited additional data regarding echocardiography assessment of torsion in PH. The advent of 3D imaging should assist further in the analysis of torsion in this setting.

## Strain by CMRI

### Myocardial tagging

CMRI tagging was a technique introduced in the late 1980s, allowing visualization of transmural myocardial involvement without the need for external physical markers. Various tagging techniques are currently available, each having different versions for improved resolution: signal-to-noise ratio (SNR); scan time; and image quality. These include basic techniques such as magnetization saturation, spatial modulation of magnetization (SPAMM), delay alternating with nutations for tailored excitation (DANTE), and complementary SPAMM (CSPAMM), and advanced techniques such as harmonic phase (HARP), displacement encoding with stimulated echoes (DENSE), and strain encoding (SENC).

The application of tagging in the evaluation of RV had been limited by the relatively thin wall. To overcome this challenge, Shehata et al. developed a fast strain-encoded (SENC) imaging, to allow direct measurement of regional function by using a free-breathing single heart beat real-time acquisition. They measured biventricular segmental and mean ventricular peak systolic longitudinal strain ( $E_{LL}$ ) as well as LV circumferential and RV tangential strains in patients with PAH and controls. Longitudinal contractility of the RV was reduced at the basal, mid, and apical levels

and tangential contractility was reduced at mid-ventricular level. Longitudinal contractility of the RV positively correlated with mPAP and PVR ( $r=0.62$  and  $r=0.77$ , respectively). Interestingly, in a subgroup of patients with normal RV function, significantly reduced RV function was noted in septal as well as free wall regions.<sup>90</sup>

### Feature tracking

A novel method of feature tracking (FT) allowing quantification of myocardial strain from CMR cine images without the need for additional sequences or images has been developed (Fig. 5).

Menezes de Siqueira et al. studied 116 patients who underwent RHC and CMRI.<sup>91</sup> Peak global longitudinal and circumferential strain and strain rates were quantified from standard cine images and association with the composite endpoint of death, lung transplantation, or worsening FC was studied. Patients were classified into three groups (no PH, PH with normal RVEF, and PH with reduced RVEF). All strain and strain rate values were reduced in the PH group with reduced RVEF. After adjustment for six clinically meaningful covariates, global longitudinal strain (GLS;  $P=0.026$ ), global longitudinal strain rate (GLSR;  $P=0.04$ ), and global circumferential strain rate (GCSR;  $P=0.01$ ) were associated with a poor outcome.

### 3D echocardiography

3D imaging by echocardiography is a relatively recent development and software has been consistently developed to incorporate specific RV measurement. Given the complexity of the RV shape, the ability to visualize the whole ventricle hopefully overcomes the limitations of assessment by 2D analyses. Measurements of RV size, ejection fraction, and mass are of particular advantage with 3D imaging.<sup>92</sup> One study showed no significant difference in average values of volume and mass between 3D echocardiography and MRI,

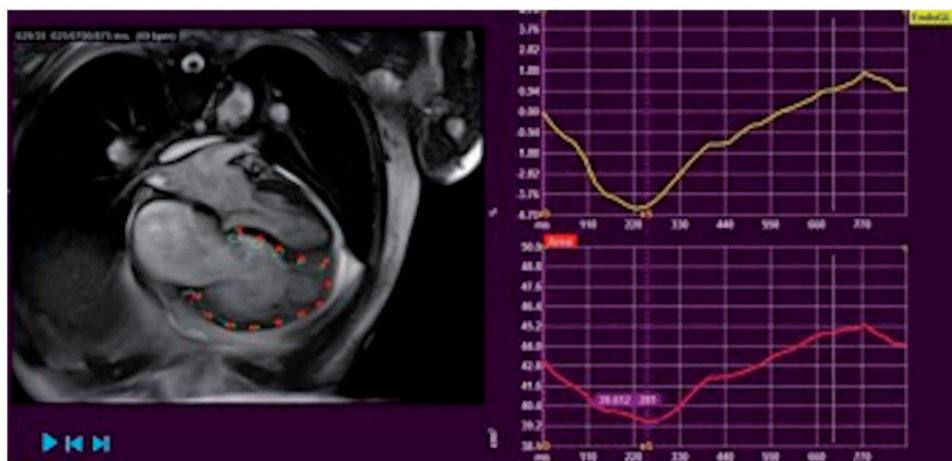


**Fig. 5.** CMRI FT images of a patient with PAH demonstrating reduced RV peak longitudinal strain.



when measured in PH and control groups; although it was acknowledged there was less inter-observer variability with MRI.<sup>41</sup> Grapsa et al. noted there was a tendency to underestimate volumes with echocardiography. A meta-analysis of RV volumes measured by 3D imaging and MRI also agreed with a tendency to underestimate by echocardiography but reported calculation of ejection fraction within 1% of the gold standard of MRI.<sup>93</sup>

3D imaging has also been used to assess right atrial size.<sup>94</sup> In this study, control and PAH groups were followed up over a one-year period. In the PAH group, increase in RA sphericity index by 0.24 predicted clinical deterioration with sensitivity 96% and specificity 90%. It is noted that a 7-second breath-hold was required to obtain 3D imaging.

Linking developments in echocardiography together, 3D imaging has been combined with strain analysis.<sup>85,95,96</sup> In one particular study a combined factor of longitudinal and circumferential strain was calculated, called area strain.<sup>95</sup> This group demonstrated improved correlation with MR calculated ejection fraction compared to longitudinal strain on its own. However, there were limitations with image acquisition, including a 21% case dropout due to suboptimal imaging in the PH group and, more notably, 36% in the control group.

## Myocardial tissue characterization and myocardial perfusion by CMRI

MRI has an advantage over echocardiography as it allows myocardial tissue characterization with contrast imaging (delayed cardiac enhancement and extracellular volume) as well as non-contrast (native T1 mapping) techniques. The myocardial changes identified in PH is likely to be a result of cardiac dysfunction but would also contribute to further deterioration of ventricular function. Furthermore, contrast-enhanced MRI allows assessment of myocardial perfusion in patients with PH.

### Delayed cardiac enhancement

Blyth et al. used contrast-enhanced CMRI to determine the presence and extent of delayed contrast enhancement (DCE) in patients with PH.<sup>97</sup> They hypothesized that myocardial abnormalities may exist in patients with PH which could be identified by contrast-enhanced CMRI and the extent of the contrast enhancement would relate to the severity of hemodynamic disturbance. DCE was present in most patients with PH studied and there were a number of statistically significant correlations between the extent of contrast enhancement seen and both invasive pulmonary hemodynamics and RV dimensions and function at CMRI including RVEDV ( $r=0.464$ ,  $P=0.02$ ), RVEF ( $r=0.762$ ,  $P<0.001$ ), RV mass index ( $r=0.679$ ,  $P<0.001$ ), and mPAP ( $r=0.672$ ,  $P<0.001$ ). The authors also found DCE to be associated with IVS bowing and concluded that this may provide a novel marker for occult septal abnormalities

directly relating to the hemodynamic stress experienced by these patients. In another study, Sanz et al. evaluated 55 patients with suspected PH.<sup>98</sup> Although the extent of DCE showed moderate to good univariate correlations with pulmonary pressures and RV volume and function, in multivariate analysis, systolic PAP was the only predictor of DCE. They concluded although presence of DCE at the RV insertion point is a common finding in PH, systolic pulmonary pressure elevation to be the main determinant of this finding. Similarly, McCann et al. found that DCE was frequently seen in patients with PH (all patients in the study) and the extent of DCE was inversely related to RV ejection fraction ( $r=-0.63$ ), RV stroke volume ( $r=-0.67$ ), and RV end-systolic volume index ( $r=-0.51$ ). Although no MRI data were available, two other patients with PAH had post-mortem histological analysis of the RV insertion points. Fibrosis was present at the RV insertion regions suggesting this may be the causal mechanism of DCE; however, there was also evidence of interstitial space expansion and a small increase in fat which may have contributed to delayed cardiac enhancement.<sup>99</sup> In a study by Freed et al., patients with RV insertion point DCE had larger RV volume index, lower RVEF, and higher mPAP. In a univariate analysis, DCE was a predictor for adverse outcomes ( $P=0.026$ ) in this population.<sup>100,101</sup>

Shehata et al. assessed DCE at the RV insertion points in relation to RV remodeling, pulmonary hemodynamics, and regional mechanics.<sup>101</sup> Out of the 32 patients diagnosed with PH, 31 demonstrated DCE. DCE was associated with pulmonary hemodynamics, reduced RV function, and reduced eccentricity index. Reduced longitudinal strain of the basal anterior septal insertion point was independently associated with DCE although the same was not observed for the posterior insertion point. The authors suggested that the two insertion regions behave differently as they are part of anatomically and functionally distinct regions, i.e. RV outflow and inflow tracts.

### T1 and extracellular volume fraction (ECV) mapping

Delayed cardiac enhancement detects focal myocardial lesions but cannot assess diffuse myocardial abnormalities. DCE also relies on visual assessment compared to the “normal” area of myocardium and requires contrast administration. Myocardial T1 mapping is a novel method of myocardial tissue characterization with the potential to identify both focal and diffuse myocardial fibrosis without the need for contrast administration (Fig. 6).

In a study by Spruijt et al., an attempt was made to characterize the myocardium in IPAH, connective tissue disease associated pulmonary hypertension (CTDPH) and CTEPH patients using native T1 mapping.<sup>102</sup> Native T1 values were assessed using regions of interest in the RV and LV free wall, RV insertion points, and the interventricular septum. In PH patients, native T1 values of the interventricular insertion regions were significantly higher than the native



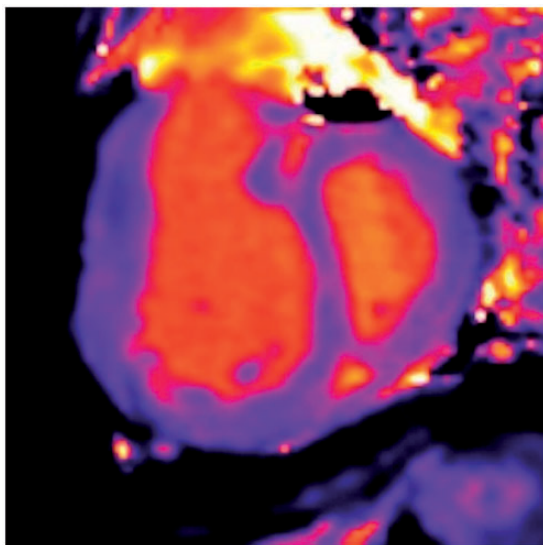


**Fig. 6.** Native T1 map of a patient with PAH demonstrating increased native T1 values in the right ventricular insertion points.

T1 values of the RV free wall, LV free wall, and interventricular septum. Native T1 values at the insertion regions were significantly related to disease severity.

In a study by Reiter et al., 58 patients with suspected PH were studied with RHC and CMRI. LV global, segmental, and ventricular insertion point (VIP) T1 times were evaluated manually and corrected for blood T1.<sup>103</sup> AHA segmentation was used to segment the LV myocardium including RV insertion points. Septal, lateral, and global VIP T1 times were significantly higher in PH than in non-PH subjects. LV eccentricity strongly correlated with VIP T1 time, which in turn was strongly associated with T1 time changes in the entire LV myocardium.

Although identification of raised native T1 times has been used to identify myocardial histological changes this has been limited due to:

1. the need for visual assessment of the insertion points;<sup>102</sup> or
2. the existing AHA segmentation of the left ventricle fails to isolate the regions of RV insertion for analysis.<sup>103</sup>

Mehta et al. attempted to develop a method of high resolution cardiac T1 mapping (accelerated and navigator gated look locker imaging for cardiac T1 estimation [ANGIE]) and compared to pre-existing modified look locker inversion recovery (MOLLI) imaging. ANGIE achieved a spatial resolution of  $1.2 \times 1.2 \text{ mm}^2$  and provided lower inter-scan variation in the RV T1 estimate compared to MOLLI ( $P < 0.05$ ).<sup>104</sup> In a study containing 12 PH patients, ten patients with heart failure with preserved ejection fraction but no PH, and ten normal volunteers, RV ECV was greater in the PH group compared to the other two. RV ECV demonstrated a linear association with increasing RVEDVI ( $P = 0.049$ ) and decreasing RVEF ( $P = 0.004$ ).<sup>105</sup>

Ana García-Álvarez et al. used an experimental model of PH (pigs with pulmonary vein banding) to assess the association between myocardial native T1 time and equilibrium contrast ECV with pulmonary hemodynamics and RV performance. Not only were the native T1 and ECV values higher at RV insertion points in banded animals compared to controls, they showed significant correlation with hemodynamics and RV-PA coupling. Interestingly ECV values were increased before overt RV dysfunction, which may offer a potential for early detection of PH.<sup>106</sup> Homsí et al. investigated LV myocardial changes associated with PAH by strain analysis and mapping techniques.<sup>107</sup> Both native T1 and ECV were higher in patients with PAH and LV longitudinal strain was impaired ( $-18$  vs.  $-23$ ,  $P < 0.01$ ). However, there was no change in LVEF. They hypothesized that due to longstanding LV under-filling, there may be LV myocardial fibrosis and LV atrophy despite preserved LVEF.

### Myocardial perfusion

Contrast-enhanced MRI enables monitoring the passage of contrast through the lungs. The passage of contrast is determined by pulmonary pressure, vascular resistance and cardiac function. Pulmonary transit time (PTT) describes the transit time of contrast between right and left ventricles while LV full width at half maximum (FWHM) and LV time to peak (TTP) contains information regarding bolus dispersion in the left ventricle. In a study by Skrok et al., patients with PH had significantly longer PTT, FWHM, and TTP than control participants. In multiple linear regression models, PTT, FWHM, and TTP were associated with mPAP and cardiac index.<sup>108</sup>

In PH, due to increased RV afterload, there is increased RV workload and RV hypertrophy. Although this demands increased RV myocardial perfusion, there may be a reduction in systolic flow in the right coronary artery in PAH. Therefore, reduced myocardial perfusion reserve may contribute to further RV dysfunction and RV failure in PAH. Vogel-Claussen et al. evaluated the relationships of RV and LV myocardial perfusion with biventricular function and pulmonary hemodynamics in PAH patients by adenosine stress perfusion MRI. Myocardial perfusion reserve indexes in the PAH group in both ventricles were lower in the PAH group compared to the scleroderma non-PH group and controls. This inversely correlated with RV workload and RVEF, concluding that reduced myocardial perfusion reserve may contribute to RV dysfunction.<sup>109</sup> Further non-invasive assessment of cardiac function under stress is discussed below.

### Cardiac function under stress by echocardiography and CMRI

#### Stress echocardiography and contractile reserve

Stress echocardiography involves the use of exercise or chemical means to increase cardiac workload. Classically

used to assess cardiac function following cardiac wall injury or for valvular function, it has identified specific roles in PH. Patients at risk of PH have been demonstrated to show abnormal responses to exercise compared to controls.<sup>110–113</sup>

Measurements taken using echocardiography, including TRV, TAPSE, S' wave velocity, strain and strain rate, chamber areas, and LVEF have all been successfully obtained during or immediately after exercise. The ability for the right ventricle to increase function in response to a stressor is termed contractile reserve. Grunig et al. subdivided a group of IPAH and CTEPH cases according to the change in PASP following a cardiopulmonary exercise test (CPET) performed with a supine bicycle.<sup>114</sup> The population that generated an increase in PASP > 30 mmHg had improved survival at four years (89% vs. 48% in the ≤ 30 mmHg group). This supports the importance of contractile reserve in prognosis. One feasibility study looked at lateral tricuspid S' wave velocity change in controls and PH patients who performed a treadmill stress test.<sup>115</sup> They demonstrated impaired change in value in the PH group (46% vs. 78% for controls). In the same study, TAPSE showed just 4% change in the PH group vs. 21% in the controls and RVFAC actually reduced by 2% in the PH group. The latter finding similar to that discussed elsewhere in this review regarding RVEF response in stress CMRI.<sup>116</sup> Nagel used stress echocardiography in a group of systemic sclerosis patients and demonstrated improved sensitivity to diagnosing PH (95.2% using stress echo vs. 72.7% at rest).<sup>117</sup> Analysis of strain by tissue Doppler imaging in healthy individuals demonstrated augmentation in values following CPET.<sup>118</sup> In the same study, additional parameters of cardiac function including S' wave velocity and TAPSE also increased. This study also demonstrated reduction in function with increasing age. A more recent study also demonstrated similar findings, again in a healthy population group.<sup>119</sup>

Dobutamine, as a chemical agent in stress echocardiography, has demonstrated use in the analysis of cardiac function in PH.<sup>120,121</sup> Domingo et al. used dobutamine to measure changes in echocardiogram-calculated mPAP and cardiac output in PH and control groups. They noted a reduction in change in cardiac output and an increase in change of mPAP in response to dobutamine in the PH group. They concluded this demonstrated a loss of both cardiac systolic and pulmonary vascular reserve in PH. Sharma et al. performed dobutamine stress echocardiograms on controls and PAH patients. They measured TAPSE and S' wave velocity of the tricuspid lateral annulus. While the values were expectedly depressed in the PH group at rest, contractile reserve was significantly more attenuated in PAH compared to controls, with change in TAPSE of 0.1 cm vs. 0.6 cm and change in S' of 4.6 cm/s vs. 11.2 cm/s, respectively.

### Exercise CMRI

CMRI is the gold standard for biventricular volume and function measurement at rest; however, there are significant challenges when CMRI is attempted during exercise.

The temporal and spatial resolution associated with CMRI is a result of image acquisition over a number of cardiac cycles, a process that depends on static cardiac position and consistent heart rate. However, during exercise, vigorous respiration causes cardiac translation. There are also difficulties in obtaining a reliable ECG signal because of magnetohydrodynamic turbulence.

As a result of these, previous investigators had focused on imaging during early recovery, at breath-hold, or at sub-maximal exercise intensities.

Holverda et al. studied a group of IPAH patients, studying stroke volume response to exercise in IPAH patients.<sup>116</sup> Cardiac function was assessed by MRI at rest and during submaximal exercise. No breath-holds were used and the temporal resolution was increased for cine and flow imaging. The MRI protocol consisted of 3 min of supine cycling. Work rate was increased in the first minute to 40% of the maximal workload as determined during exercise testing. In healthy controls, all cardiac parameters significantly increased with the exception of RVEDV and LVEDB. Patients with IPAH were not able to significantly increase SV, thus CO was augmented by an increase in heart rate only. In the patient group, RVEDV increased and LVEDV significantly decreased during exercise. The group identified that in healthy controls the increased stroke volume during exercise was due to a fall in ESVs suggesting an augmentation of SV due to increased myocardial contractility. They also found that there is reduction in RVEF during exercise in IPAH patients providing evidence of RV failure manifestation during exercise.

La Gerche et al. developed a method of CMRI acquisition and analysis enabling CINE images to be acquired during intense exercise without ECG gating with retrospective synchronization for cardiac and respiratory cycles. During the pilot phases, they looked at feasibility of real-time-ungated imaging (RT-ungated CMRI) compared with standard ECG-gated imaging and assessed these against the invasive FICK method. Cardiac output determined by RT-ungated CMRI proved accurate against the direct Fick method with excellent agreement which was highly reproducible during a second bout of maximal exercise.<sup>122</sup>

The authors concluded that when RT-ungated CMRI is combined with post-hoc analysis incorporating compensation for respiratory motion, highly reproducible and accurate biventricular volumes can be measured during maximal exercise. In an exercise CMRI study (with simultaneous RHC) of CTEPH, patients and patients with normalized mPAP post PEA (and healthy controls) were studied. Resting RVEF was reduced in CTEPH but not in post-PEA patients.<sup>123</sup> Interestingly, peak exercise RVEF was reduced in both CTEPH and post-PEA groups. Pulmonary arterial compliance was defined as the ratio between RV SV and PAP pressure. Exercise led to reduction of pulmonary arterial compliance in all groups. In post-PEA patients, a PDE-5 inhibitor did not affect resting RHC and CMR measurements but decreased the mPAP/cardiac output slope and increased peak exercise RVEF.

**Table 1.** Advantages and disadvantages of Echocardiography vs Cardiac MRI

	Advantages	Disadvantages
Echocardiography	Accessibility Doppler-derived pressure Stress studies Not limited by implantable devices/foreign bodies Not claustrophobic Safe	Patient habitus-dependent Operator-dependent Angle-dependent Accuracy and precision Specialist techniques require skilled technician
MRI	Gold standard Safe Non-operator-dependent Myocardial tissue characterization Myocardial perfusion	Specialist technicians to obtain correct phase Limitation on patient habitus Metallic implants Claustrophobia Expense Accessibility No pressures

**Table 2.** Suggested key Echocardiography and Cardiac MRI measurements at diagnosis and follow-up

Suggested key measurements	Echocardiography	MRI	Also consider
Initial	TRV/TRPG RAP (by IVC) S' wave velocity of the lateral tricuspid annulus Chamber sizes RVFAC TAPSE RV wall thickness LV function	RV and LV volumes (EDV, ESV, SV) RV and LV mass and mass index RVEF and LVEF LA volume Tissue characterization – DCE and/or T1 mapping	Stress echo TRV/TRPG in borderline cases RVEF by 3D echo strain analysis by echo or CMRI
Follow-up	TRV/TRPG RAP (by IVC) Chamber sizes RVFAC	RV and LV volumes (EDV, ESV, SV) RV and LV mass and mass index RVEF and LVEF	RVEF by 3D echo strain analysis by echo or CMRI

## Summary

Echocardiography is an established imaging modality that brings a wealth of information on cardiac function. Perhaps the primary advantage of echocardiography has always been accessibility and safety. However, developments in hardware and software have allowed this modality to grow from a basic projection of a simple line of interest to real time 3D capture. While the general evidence would agree MRI is required to provide gold standard measurements of volume, echocardiography appears to be catching up with image quality, precision, and accuracy. The development of speckle tracking—unique to echo, and stress echocardiography—which is already well established, add to its attraction. However, developments in MRI catheterization, which involves RHC performed inside a MRI scanner using MRI instead of fluoroscopic guidance, allow hemodynamic, structural, and functional assessment without radiation and are likely to play an important role in cardiopulmonary disease assessment in the future.<sup>124</sup> There is also ongoing work

on estimating PAP from a combination of MRI indices. Using LA volume and cardiac output using MRI, PVR could be estimated.<sup>125</sup> Real-time CMRI promises a robust method for patients who are unable to breath-hold and in patients with arrhythmias where a good-quality ECG cannot be achieved.<sup>126</sup> These changes may further consolidate the position of CMRI as the gold standard of investigating patients with PH.

However, at present, rather than to compete with MRI, these two modalities should be looked upon as complementary. The ability to obtain non-invasive reliable cardiac assessment should always focus on the benefit to the patient with this rare condition. The closer echocardiography gets to correlation with proven MR measurements, the greater its use in the screening, initial diagnosis, and subsequent follow-up of patients with PH. The advantages and disadvantages of these two imaging modalities are summarized in Table 1. Although we have discussed a number of echocardiography and MRI variables during this review, at present we suggest that established parameters should be



measured at diagnosis and as an adjunct to clinical examination, NTproBNP and 6MWT at follow-up visits. The suggested measurements are summarized in Table 2.

### Conflict of interest

The authors declare that there is no conflict of interest.

### Funding

This research received no specific grant from any funding agency in the public, commercial, or not-for-profit sectors.

### References

1. D'Alto M, Scognamiglio G, Dimopoulos K, et al. Right heart and pulmonary vessels structure and function. *Echocardiography* 2015; 32(Suppl. 1): S3–10.
2. Naeije R, Brimioulle S and Dewachter L. Biomechanics of the right ventricle in health and disease (2013 Grover Conference series). *Pulm Circ* 2014; 4(3): 395–406.
3. Vanderpool RR, Pinsky MR, Naeije R, et al. RV-pulmonary arterial coupling predicts outcome in patients referred for pulmonary hypertension. *Heart* 2015; 101(1): 37–43.
4. Guazzi M, Naeije R, Arena R, et al. Echocardiography of right ventriculoarterial coupling combined with cardiopulmonary exercise testing to predict outcome in heart failure. *Chest* 2015; 148(1): 226–234.
5. Ho SY and Nihoyannopoulos P. Anatomy, echocardiography, and normal right ventricular dimensions. *Heart* 2006; 92(Suppl. 1): i2–13.
6. Apostolakis S and Konstantinides S. The right ventricle in health and disease: insights into physiology, pathophysiology and diagnostic management. *Cardiology* 2012; 121(4): 263–273.
7. Hertz C and Edler I. Die Registrierung von Herzwandbewegungen mit Hilfe des Ultraschall-Impulsverfahrens. *Acta Acustica united with Acustica* 1956; 6(4): 361–364.
8. Roberts JD and Forfia PR. Diagnosis and assessment of pulmonary vascular disease by Doppler echocardiography. *Pulm Circ* 2011; 1(2): 160–181.
9. Bossone E, D'Andrea A, D'Alto M, et al. Echocardiography in pulmonary arterial hypertension: from diagnosis to prognosis. *J Am Soc Echocardiogr* 2013; 26(1): 1–14.
10. Grünig E and Peacock AJ. Imaging the heart in pulmonary hypertension: an update. *Eur Respir Rev* 2015; 24(138): 653–664.
11. Lang RM, Badano LP, Mor-Avi V, et al. Recommendations for cardiac chamber quantification by echocardiography in adults: an update from the American Society of Echocardiography and the European Association of Cardiovascular Imaging. *Eur Heart J Cardiovasc Imaging* 2015; 16(3): 233–270.
12. Howard LS, Grapsa J, Dawson D, et al. Echocardiographic assessment of pulmonary hypertension: standard operating procedure. *Eur Respir Rev* 2012; 21(125): 239–248.
13. Wollschlager H. [3D echocardiography. Mathematical principles and technical realization]. *Herz* 1995; 20(4): 225–235.
14. Greenleaf JF, Belohlavek M, Gerber TC, et al. Multidimensional visualization in echocardiography: an introduction. *Mayo Clin Proc* 1993; 68(3): 213–220.
15. Vasko SD, Goldberg SJ, Requarth JA, et al. Factors affecting accuracy of in vitro valvar pressure gradient estimates by Doppler ultrasound. *Am J Cardiol* 1984; 54(7): 893–896.
16. Soliman OI, Krenning BJ, Geleijnse ML, et al. A comparison between QLAB and TomTec full volume reconstruction for real time three-dimensional echocardiographic quantification of left ventricular volumes. *Echocardiography* 2007; 24(9): 967–974.
17. Voigt J-U, Pedrizzetti G, Lysyansky P, et al. Definitions for a common standard for 2D speckle tracking echocardiography: consensus document of the EACVI/ASE/Industry Task Force to standardize deformation imaging. *European Heart Journal - Cardiovascular Imaging* 2015; 16(1): 1–11.
18. Lang RM, Badano LP, Mor-Avi V, et al. Recommendations for cardiac chamber quantification by echocardiography in adults: an update from the American Society of Echocardiography and the European Association of Cardiovascular Imaging. *J Am Soc Echocardiogr* 2015; 28(1): 1–39.e14.
19. Ghio S, Pazzano AS, Klersy C, et al. Clinical and prognostic relevance of echocardiographic evaluation of right ventricular geometry in patients with idiopathic pulmonary arterial hypertension. *Am J Cardiol* 2011; 107(4): 628–632.
20. Anavekar NS, Gerson D, Skali H, et al. Two-dimensional assessment of right ventricular function: an echocardiographic-MRI correlative study. *Echocardiography* 2007; 24(5): 452–456.
21. Zornoff LA, Skali H, Pfeffer MA, et al. Right ventricular dysfunction and risk of heart failure and mortality after myocardial infarction. *J Am Coll Cardiol* 2002; 39(9): 1450–1455.
22. Kaul S, Tei C, Hopkins JM, et al. Assessment of right ventricular function using two-dimensional echocardiography. *Am Heart J* 1984; 107(3): 526–531.
23. Forfia PR, Fisher MR, Mathai SC, et al. Tricuspid annular displacement predicts survival in pulmonary hypertension. *Am J Respir Crit Care Med* 2006; 174(9): 1034–1041.
24. Ghio S, Klersy C, Magrini G, et al. Prognostic relevance of the echocardiographic assessment of right ventricular function in patients with idiopathic pulmonary arterial hypertension. *Int J Cardiol* 2010; 140(3): 272–278.
25. Wong DJ, Sampat U, Gibson MA, et al. Tricuspid annular plane systolic excursion in chronic thromboembolic pulmonary hypertension before and after pulmonary thromboendarterectomy. *Echocardiography* 2016; 33(12): 1805–1809.
26. van Kessel M, Seaton D, Chan J, et al. Prognostic value of right ventricular free wall strain in pulmonary hypertension patients with pseudo-normalized tricuspid annular plane systolic excursion values. *Int J Cardiovasc Imaging* 2016; 32(6): 905–912.
27. Sivak JA, Raina A and Forfia PR. Assessment of the physiologic contribution of right atrial function to total right heart function in patients with and without pulmonary arterial hypertension. *Pulm Circ* 2016; 6(3): 322–328.
28. Asmer I, Adawi S, Ganaem M, et al. Right ventricular outflow tract systolic excursion: a novel echocardiographic parameter of right ventricular function. *Eur Heart J Cardiovasc Imaging* 2012; 13(10): 871–877.
29. Alsoos F, Almobarak M and Shebli H. Right ventricular outflow tract systolic excursion: a useful method for determining right ventricular systolic function. *J Echocardiogr* 2014; 12(4): 151–158.



30. Lindqvist P, Henein M and Kazzam E. Right ventricular out-flow-tract fractional shortening: an applicable measure of right ventricular systolic function. *Eur J Echocardiogr* 2003; 4(1): 29–35.
31. Fisher MR, Forfia PR, Chamera E, et al. Accuracy of Doppler echocardiography in the hemodynamic assessment of pulmonary hypertension. *Am J Respir Crit Care Med* 2009; 179(7): 615–621.
32. Medvedofsky D, Aronson D, Gomberg-Maitland M, et al. Tricuspid regurgitation progression and regression in pulmonary arterial hypertension: implications for right ventricular and tricuspid valve apparatus geometry and patients outcome. *Eur Heart J Cardiovasc Imaging* 2017; 18(1): 86–94.
33. Meluzin J, Spinarova L, Bakala J, et al. Pulsed Doppler tissue imaging of the velocity of tricuspid annular systolic motion; a new, rapid, and non-invasive method of evaluating right ventricular systolic function. *Eur Heart J* 2001; 22(4): 340–348.
34. Rudski LG, Lai WW, Afilalo J, et al. Guidelines for the echocardiographic assessment of the right heart in adults: a report from the American Society of Echocardiography endorsed by the European Association of Echocardiography, a registered branch of the European Society of Cardiology, and the Canadian Society of Echocardiography. *J Am Soc Echocardiogr* 2010; 23(7): 685–713; quiz 86–88.
35. Tei C, Dujardin KS, Hodge DO, et al. Doppler echocardiographic index for assessment of global right ventricular function. *J Am Soc Echocardiogr* 1996; 9(6): 838–847.
36. Yeo TC, Dujardin KS, Tei C, et al. Value of a Doppler-derived index combining systolic and diastolic time intervals in predicting outcome in primary pulmonary hypertension. *Am J Cardiol* 1998; 81(9): 1157–1161.
37. Cheung MM, Smallhorn JF, Redington AN, et al. The effects of changes in loading conditions and modulation of inotropic state on the myocardial performance index: comparison with conductance catheter measurements. *Eur Heart J* 2004; 25(24): 2238–2242.
38. Grothues F, Moon JC, Bellenger NG, et al. Interstudy reproducibility of right ventricular volumes, function, and mass with cardiovascular magnetic resonance. *Am Heart J* 2004; 147(2): 218–223.
39. Semelka RC, Tomei E, Wagner S, et al. Interstudy reproducibility of dimensional and functional measurements between cine magnetic resonance studies in the morphologically abnormal left ventricle. *Am Heart J* 1990; 119(6): 1367–1373.
40. Beerbaum P, Korperich H, Barth P, et al. Noninvasive quantification of left-to-right shunt in pediatric patients: phase-contrast cine magnetic resonance imaging compared with invasive oximetry. *Circulation* 2001; 103(20): 2476–2482.
41. Grapsa J, O'Regan DP, Pavlopoulos H, et al. Right ventricular remodelling in pulmonary arterial hypertension with three-dimensional echocardiography: comparison with cardiac magnetic resonance imaging. *Eur J Echocardiogr* 2010; 11(1): 64–73.
42. van Wolferen SA, Marcus JT, Boonstra A, et al. Prognostic value of right ventricular mass, volume, and function in idiopathic pulmonary arterial hypertension. *Eur Heart J* 2007; 28(10): 1250–1257.
43. Campo A, Mathai SC, Le Pavec J, et al. Hemodynamic predictors of survival in scleroderma-related pulmonary arterial hypertension. *Am J Respir Crit Care Med* 2010; 182(2): 252–260.
44. van Wolferen SA, van de Veerdonk MC, Mauritz GJ, et al. Clinically significant change in stroke volume in pulmonary hypertension. *Chest* 2011; 139(5): 1003–1009.
45. van de Veerdonk MC, Kind T, Marcus JT, et al. Progressive right ventricular dysfunction in patients with pulmonary arterial hypertension responding to therapy. *J Am Coll Cardiol* 2011; 58(24): 2511–2519.
46. Yamada Y, Okuda S, Kataoka M, et al. Prognostic value of cardiac magnetic resonance imaging for idiopathic pulmonary arterial hypertension before initiating intravenous prostacyclin therapy. *Circ J* 2012; 76(7): 1737–1743.
47. Mauritz GJ, Kind T, Marcus JT, et al. Progressive changes in right ventricular geometric shortening and long-term survival in pulmonary arterial hypertension. *Chest* 2012; 141(4): 935–943.
48. Sanz J, Kuschner P, Rius T, et al. Pulmonary arterial hypertension: noninvasive detection with phase-contrast MR imaging. *Radiology* 2007; 243(1): 70–79.
49. Mousseaux E, Tasu JP, Jolivet O, et al. Pulmonary arterial resistance: noninvasive measurement with indexes of pulmonary flow estimated at velocity-encoded MR imaging—preliminary experience. *Radiology* 1999; 212(3): 896–902.
50. Helderman F, Mauritz GJ, Andringa KE, et al. Early onset of retrograde flow in the main pulmonary artery is a characteristic of pulmonary arterial hypertension. *J Magn Reson Imaging* 2011; 33(6): 1362–1368.
51. Sanz J, Kariisa M, Dellegrattaglie S, et al. Evaluation of pulmonary artery stiffness in pulmonary hypertension with cardiac magnetic resonance. *JACC Cardiovasc Imaging* 2009; 2(3): 286–295.
52. Brewis MJ, Bellofiore A, Vanderpool RR, et al. Imaging right ventricular function to predict outcome in pulmonary arterial hypertension. *Int J Cardiol* 2016; 218: 206–211.
53. Peacock AJ, Crawley S, McLure L, et al. Changes in right ventricular function measured by cardiac magnetic resonance imaging in patients receiving pulmonary arterial hypertension-targeted therapy: the EURO-MR study. *Circ Cardiovasc Imaging* 2014; 7(1): 107–114.
54. Roeleveld RJ, Marcus JT, Faes TJ, et al. Interventricular septal configuration at mr imaging and pulmonary arterial pressure in pulmonary hypertension. *Radiology* 2005; 234(3): 710–717.
55. Dellegrattaglie S, Sanz J, Poon M, et al. Pulmonary hypertension: accuracy of detection with left ventricular septal-to-free wall curvature ratio measured at cardiac MR. *Radiology* 2007; 243(1): 63–69.
56. Beyar R, Dong SJ, Smith ER, et al. Ventricular interaction and septal deformation: a model compared with experimental data. *Am J Physiol* 1993; 265(6 Pt 2): H2044–2056.
57. Ryan T, Petrovic O, Dillon JC, et al. An echocardiographic index for separation of right ventricular volume and pressure overload. *J Am Coll Cardiol* 1985; 5(4): 918–927.
58. Puwanant S, Park M, Popović ZB, et al. Ventricular geometry, strain, and rotational mechanics in pulmonary hypertension. *Circulation* 2010; 121(2): 259–266.
59. Willens HJ, Fertel DP, Qin J, et al. Effects of age and pulmonary arterial hypertension on the different phases of right atrial function. *Int J Cardiovasc Imaging* 2008; 24(7): 703–710.

60. Lambertz H, Krebs W, Soeding S, et al. [Determination of the size of the right atrium in patients with pulmonary hypertension using 2-dimensional echocardiography]. *Z Kardiol* 1984; 73(10): 646–653.
61. Gaynor SL, Maniar HS, Bloch JB, et al. Right atrial and ventricular adaptation to chronic right ventricular pressure overload. *Circulation* 2005; 112(9 Suppl): I212–218.
62. Crawley SF, Johnson MK, Dargie HJ, et al. LA volume by CMR distinguishes idiopathic from pulmonary hypertension due to HFpEF. *JACC Cardiovasc Imaging* 2013; 6(10): 1120–1121.
63. Dandel M, Lehmkuhl H, Knosalla C, et al. Strain and strain rate imaging by echocardiography - basic concepts and clinical applicability. *Curr Cardiol Rev* 2009; 5(2): 133–148.
64. Reisner SA, Lysyansky P, Agmon Y, et al. Global longitudinal strain: a novel index of left ventricular systolic function. *J Am Soc Echocardiogr* 2004; 17(6): 630–633.
65. Leitman M, Lysyansky P, Sidenko S, et al. Two-dimensional strain-a novel software for real-time quantitative echocardiographic assessment of myocardial function. *J Am Soc Echocardiogr* 2004; 17(10): 1021–1029.
66. Helle-Valle T, Crosby J, Edvardsen T, et al. New noninvasive method for assessment of left ventricular rotation: speckle tracking echocardiography. *Circulation* 2005; 112(20): 3149–3156.
67. Amundsen BH, Helle-Valle T, Edvardsen T, et al. Noninvasive myocardial strain measurement by speckle tracking echocardiography: validation against sonomicrometry and tagged magnetic resonance imaging. *J Am Coll Cardiol* 2006; 47(4): 789–793.
68. Rajdev S, Nanda NC, Patel V, et al. Tissue Doppler assessment of longitudinal right and left ventricular strain and strain rate in pulmonary artery hypertension. *Echocardiography* 2006; 23(10): 872–879.
69. Borges AC, Knebel F, Eddicks S, et al. Right ventricular function assessed by two-dimensional strain and tissue Doppler echocardiography in patients with pulmonary arterial hypertension and effect of vasodilator therapy. *Am J Cardiol* 2006; 98(4): 530–534.
70. Teske AJ, De Boeck BW, Olimulder M, et al. Echocardiographic assessment of regional right ventricular function: a head-to-head comparison between 2-dimensional and tissue Doppler-derived strain analysis. *J Am Soc Echocardiogr* 2008; 21(3): 275–283.
71. Filusch A, Mereles D, Gruenig E, et al. Strain and strain rate echocardiography for evaluation of right ventricular dysfunction in patients with idiopathic pulmonary arterial hypertension. *Clin Res Cardiol* 2010; 99(8): 491–498.
72. Sachdev A, Villarraga HR, Frantz RP, et al. Right ventricular strain for prediction of survival in patients with pulmonary arterial hypertension. *Chest* 2011; 139(6): 1299–1309.
73. Haack ML, Scherptong RW, Marsan NA, et al. Prognostic value of right ventricular longitudinal peak systolic strain in patients with pulmonary hypertension. *Circ Cardiovasc Imaging* 2012; 5(5): 628–636.
74. Rajagopal S, Forsha DE, Risum N, et al. Comprehensive assessment of right ventricular function in patients with pulmonary hypertension with global longitudinal peak systolic strain derived from multiple right ventricular views. *J Am Soc Echocardiogr* 2014; 27(6): 657–665.e3.
75. Park JH, Kusunose K, Kwon DH, et al. Relationship between right ventricular longitudinal strain, invasive hemodynamics, and functional assessment in pulmonary arterial hypertension. *Korean Circ J* 2015; 45(5): 398–407.
76. Park JH, Park MM, Farha S, et al. Impaired global right ventricular longitudinal strain predicts long-term adverse outcomes in patients with pulmonary arterial hypertension. *J Cardiovasc Ultrasound* 2015; 23(2): 91–99.
77. Li Y, Wang Y, Ye X, et al. Clinical study of right ventricular longitudinal strain for assessing right ventricular dysfunction and hemodynamics in pulmonary hypertension. *Medicine (Baltimore)* 2016; 95(50): e5668.
78. Teske AJ, Prakken NH, De Boeck BW, et al. Echocardiographic tissue deformation imaging of right ventricular systolic function in endurance athletes. *Eur Heart J* 2009; 30(8): 969–977.
79. Marston N, Brown JP, Olson N, et al. Right ventricular strain before and after pulmonary thromboendarterectomy in patients with chronic thromboembolic pulmonary hypertension. *Echocardiography* 2015; 32(7): 1115–1121.
80. Broch K, Murbraech K, Ragnarsson A, et al. Echocardiographic evidence of right ventricular functional improvement after balloon pulmonary angioplasty in chronic thromboembolic pulmonary hypertension. *J Heart Lung Transplant* 2016; 35(1): 80–86.
81. Li Y, Xie M, Wang X, et al. Right ventricular regional and global systolic function is diminished in patients with pulmonary arterial hypertension: a 2-dimensional ultrasound speckle tracking echocardiography study. *Int J Cardiovasc Imaging* 2013; 29(3): 545–551.
82. Querejeta Roca G, Campbell P, Claggett B, et al. Right atrial function in pulmonary arterial hypertension. *Circ Cardiovasc Imaging* 2015; 8(11): e003521; discussion e003521.
83. D'Andrea A, Naeije R, Grunig E, et al. Echocardiography of the pulmonary circulation and right ventricular function: exploring the physiologic spectrum in 1,480 normal subjects. *Chest* 2014; 145(5): 1071–1078.
84. Fukuda Y, Tanaka H, Ryo-Koriyama K, et al. Comprehensive functional assessment of right-sided heart using speckle tracking strain for patients with pulmonary hypertension. *Echocardiography* 2016; 33(7): 1001–1008.
85. Vitarelli A, Mangieri E, Terzano C, et al. Three-dimensional echocardiography and 2D-3D speckle-tracking imaging in chronic pulmonary hypertension: diagnostic accuracy in detecting hemodynamic signs of right ventricular (RV) failure. *J Am Heart Assoc* 2015; 4(3): e001584.
86. Haack ML, Hoke U, Marsan NA, et al. Impact of right ventricular dyssynchrony on left ventricular performance in patients with pulmonary hypertension. *Int J Cardiovasc Imaging* 2014; 30(4): 713–720.
87. Badagliacca R, Poscia R, Pezzuto B, et al. Right ventricular dyssynchrony in idiopathic pulmonary arterial hypertension: determinants and impact on pump function. *J Heart Lung Transplant* 2015; 34(3): 381–389.
88. Badagliacca R, Reali M, Poscia R, et al. Right intraventricular dyssynchrony in idiopathic, heritable, and anorexigen-induced pulmonary arterial hypertension: clinical impact and reversibility. *JACC Cardiovasc Imaging* 2015; 8(6): 642–652.
89. Notomi Y, Lysyansky P, Setser RM, et al. Measurement of ventricular torsion by two-dimensional ultrasound

- speckle tracking imaging. *J Am Coll Cardiol* 2005; 45(12): 2034–2041.
90. Shehata ML, Basha TA, Tantawy WH, et al. Real-time single-heartbeat fast strain-encoded imaging of right ventricular regional function: normal versus chronic pulmonary hypertension. *Magn Reson Med* 2010; 64(1): 98–106.
  91. de Siqueira ME, Pozo E, Fernandes VR, et al. Characterization and clinical significance of right ventricular mechanics in pulmonary hypertension evaluated with cardiovascular magnetic resonance feature tracking. *J Cardiovasc Magn Reson* 2016; 18(1): 39.
  92. Knight DS, Grasso AE, Quail MA, et al. Accuracy and reproducibility of right ventricular quantification in patients with pressure and volume overload using single-beat three-dimensional echocardiography. *J Am Soc Echocardiogr* 2015; 28(3): 363–374.
  93. Shimada YJ, Shiota M, Siegel RJ, et al. Accuracy of right ventricular volumes and function determined by three-dimensional echocardiography in comparison with magnetic resonance imaging: a meta-analysis study. *J Am Soc Echocardiogr* 2010; 23(9): 943–953.
  94. Grapsa J, Gibbs JS, Cabrita IZ, et al. The association of clinical outcome with right atrial and ventricular remodelling in patients with pulmonary arterial hypertension: study with real-time three-dimensional echocardiography. *Eur Heart J Cardiovasc Imaging* 2012; 13(8): 666–672.
  95. Smith BC, Dobson G, Dawson D, et al. Three-dimensional speckle tracking of the right ventricle: toward optimal quantification of right ventricular dysfunction in pulmonary hypertension. *J Am Coll Cardiol* 2014; 64(1): 41–51.
  96. Pigatto E, Peluso D, Zanatta E, et al. Evaluation of right ventricular function performed by 3D-echocardiography in scleroderma patients. *Reumatismo* 2015; 66(4): 259–263.
  97. Blyth KG, Groenning BA, Martin TN, et al. Contrast enhanced-cardiovascular magnetic resonance imaging in patients with pulmonary hypertension. *Eur Heart J* 2005; 26(19): 1993–1999.
  98. Sanz J, Dellegrottaglie S, Kariisa M, et al. Prevalence and correlates of septal delayed contrast enhancement in patients with pulmonary hypertension. *Am J Cardiol* 2007; 100(4): 731–735.
  99. McCann GP, Beek AM, Vonk-Noordegraaf A, et al. Delayed contrast-enhanced magnetic resonance imaging in pulmonary arterial hypertension. *Circulation* 2005; 112(16): e268.
  100. Freed BH, Gomberg-Maitland M, Chandra S, et al. Late gadolinium enhancement cardiovascular magnetic resonance predicts clinical worsening in patients with pulmonary hypertension. *J Cardiovasc Magn Reson* 2012; 14: 11.
  101. Shehata ML, Lossnitzer D, Skrok J, et al. Myocardial delayed enhancement in pulmonary hypertension: pulmonary hemodynamics, right ventricular function, and remodeling. *AJR Am J Roentgenol* 2011; 196(1): 87–94.
  102. Spruijt OA, Vissers L, Bogaard HJ, et al. Increased native T1-values at the interventricular insertion regions in precapillary pulmonary hypertension. *Int J Cardiovasc Imaging* 2016; 32(3): 451–459.
  103. Reiter U, Reiter G, Kovacs G, et al. Native myocardial T1 mapping in pulmonary hypertension: correlations with cardiac function and hemodynamics. *Eur Radiol* 2017; 27(1): 157–166.
  104. Mehta BB, Chen X, Bilchick KC, et al. Accelerated and navigator-gated look-locker imaging for cardiac T1 estimation (ANGIE): Development and application to T1 mapping of the right ventricle. *Magn Reson Med* 2015; 73(1): 150–160.
  105. Mehta BB, Auger DA, Gonzalez JA, et al. Detection of elevated right ventricular extracellular volume in pulmonary hypertension using Accelerated and Navigator-Gated Look-Locker Imaging for Cardiac T1 Estimation (ANGIE) cardiovascular magnetic resonance. *J Cardiovasc Magn Reson* 2015; 17: 110.
  106. Garcia-Alvarez A, Garcia-Lunar I, Pereda D, et al. Association of myocardial T1-mapping CMR with hemodynamics and RV performance in pulmonary hypertension. *JACC Cardiovasc Imaging* 2015; 8(1): 76–82.
  107. Homsí R, Luetkens JA, Skowasch D, et al. Left ventricular myocardial fibrosis, atrophy, and impaired contractility in patients with pulmonary arterial hypertension and a preserved left ventricular function: a cardiac magnetic resonance study. *J Thorac Imaging* 2017; 32(1): 36–42.
  108. Skrok J, Shehata ML, Mathai S, et al. Pulmonary arterial hypertension: MR imaging-derived first-pass bolus kinetic parameters are biomarkers for pulmonary hemodynamics, cardiac function, and ventricular remodeling. *Radiology* 2012; 263(3): 678–687.
  109. Vogel-Claussen J, Skrok J, Shehata ML, et al. Right and left ventricular myocardial perfusion reserves correlate with right ventricular function and pulmonary hemodynamics in patients with pulmonary arterial hypertension. *Radiology* 2011; 258(1): 119–127.
  110. Grünig E, Janssen B, Mereles D, et al. Abnormal pulmonary artery pressure response in asymptomatic carriers of primary pulmonary hypertension gene. *Circulation* 2000; 102(10): 1145–1150.
  111. Grünig E, Weissmann S, Ehlken N, et al. Stress Doppler echocardiography in relatives of patients with idiopathic and familial pulmonary arterial hypertension: results of a multicenter European analysis of pulmonary artery pressure response to exercise and hypoxia. *Circulation* 2009; 119(13): 1747–1757.
  112. Kovacs G, Maier R, Aberer E, et al. Assessment of pulmonary arterial pressure during exercise in collagen vascular disease: echocardiography vs right-sided heart catheterization. *Chest* 2010; 138(2): 270–278.
  113. Kusunose K, Yamada H, Hotchi J, et al. Prediction of future overt pulmonary hypertension by 6-min walk stress echocardiography in patients with connective tissue disease. *J Am Coll Cardiol* 2015; 66(4): 376–384.
  114. Grünig E, Tiede H, Enyimayew EO, et al. Assessment and prognostic relevance of right ventricular contractile reserve in patients with severe pulmonary hypertension. *Circulation* 2013; 128(18): 2005–2015.
  115. Almeida AR, Loureiro MJ, Lopes L, et al. Echocardiographic assessment of right ventricular contractile reserve in patients with pulmonary hypertension. *Rev Port Cardiol* 2014; 33(3): 155–163.
  116. Holverda S, Gan CT, Marcus JT, et al. Impaired stroke volume response to exercise in pulmonary arterial hypertension. *J Am Coll Cardiol* 2006; 47(8): 1732–1733.
  117. Nagel C, Henn P, Ehlken N, et al. Stress Doppler echocardiography for early detection of systemic sclerosis-associated

- pulmonary arterial hypertension. *Arthritis Res Ther* 2015; 17: 165.
118. Chia EM, Hsieh CH, Pham P, et al. Changes in right ventricular function with exercise in healthy subjects: optimal parameters and effects of gender and age. *J Am Soc Echocardiogr* 2015; 28(12): 1441–1451.e1.
  119. D'Alto M, Pavelescu A, Argiento P, et al. Echocardiographic assessment of right ventricular contractile reserve in healthy subjects. *Echocardiography* 2017; 34(1): 61–68.
  120. Domingo E, Grignola JC, Aguilar R, et al. Impairment of pulmonary vascular reserve and right ventricular systolic reserve in pulmonary arterial hypertension. *BMC Pulm Med* 2014; 14: 69.
  121. Sharma T, Lau EM, Choudhary P, et al. Dobutamine stress for evaluation of right ventricular reserve in pulmonary arterial hypertension. *Eur Respir J* 2015; 45(3): 700–708.
  122. La Gerche A, Claessen G, Van de Bruaene A, et al. Cardiac MRI: a new gold standard for ventricular volume quantification during high-intensity exercise. *Circ Cardiovasc Imaging* 2013; 6(2): 329–338.
  123. Claessen G, La Gerche A, Dymarkowski S, et al. Pulmonary vascular and right ventricular reserve in patients with normalized resting hemodynamics after pulmonary endarterectomy. *J Am Heart Assoc* 2015; 4(3): e001602.
  124. Rogers T, Ratnayaka K and Lederman RJ. MRI catheterization in cardiopulmonary disease. *Chest* 2014; 145(1): 30–36.
  125. Swift AJ, Rajaram S, Hurdman J, et al. Noninvasive estimation of PA pressure, flow, and resistance with CMR imaging: derivation and prospective validation study from the ASPIRE registry. *JACC Cardiovasc Imaging* 2013; 6(10): 1036–1047.
  126. Bauer RW, Radtke I, Block KT, et al. True real-time cardiac MRI in free breathing without ECG synchronization using a novel sequence with radial k-space sampling and balanced SSFP contrast mode. *Int J Cardiovasc Imaging* 2013; 29(5): 1059–1067.